Controller Design and Implementation of a Medium Voltage (13.8 kV) Modular Multi-Level Converter for Asynchronous Microgrids

Dingrui Li[1], Xingxuan Huang[1], Shiqi Ji[1], Cheng Nie[1], Fred Wang[1,2], and Leon M. Tolbert [1,2]

[1] Min H. Kao Department of Electrical Engineering & Computer Science,
The University of Tennessee, Knoxville, TN, USA
[2]Oak Ridge National Laboratory, Oak Ridge, TN, USA

dli35@vols.utk.edu

***Abstract*— Asynchronous microgrid with power condition system (PCS) converter is a potential future application area of medium voltage converters. However, there has been only limited research focusing on actual implementation of PCS converters. This paper describes the controller development of a 13.8 kV, silicon carbide (SiC) MOSFET-based dc/ac four-wire modular multi-level converter (MMC) for an asynchronous microgrid considering grid requirements. Control architecture and detailed central and phase controller functions are discussed. Experimental results under balanced and unbalanced load conditions are demonstrated.**

Keywords—Controller design, medium voltage converter, asynchronous microgrid, modular multi-level converter

I. INTRODUCTION

Due to the recent development of high voltage wide bandgap (WBG) semiconductor devices, medium voltage (MV) converters have become more feasible for a wider array of grid applications [1-6], especially microgrids. MV converters have two main types of applications in microgrids. The first one is to interface with distributed energy resources (DERs) including wind turbines [1-3], battery energy storage systems [4], solar power, etc. The second one is to work as interfaces between different grids to form a new system [5-7]. In the second type applications, MV solid state transformers (SSTs) have been used to form dc microgrids [5-6]. In addition to SST, recently, other ac/dc, dc/ac converters have been proposed to connect main grids with ac microgrids, such as illustrated in Fig. 1. This connection structure is also called asynchronous microgrid [7].

In an asynchronous microgrid, interface PCS converter supports normal system operations as well as decouples the dynamics between the two systems [8]. PCS converter consists of two back-to-back connected ac/dc and dc/ac MV converters. In the microgrid grid-connected operation, the grid-side converter regulates dc-link voltage, and the microgrid side converter supports microgrid voltage and frequency. In the islanded operation, only the microgrid side converter operates to regulate dc-link voltage and compensate reactive power. Potential grid benefits of an asynchronous microgrid have been discussed in several papers, which include better mode transition capability [9], fault isolation [10], etc. However, there are only a few papers focusing on the realization of PCS converters. Reference [9] demonstrated grid level controller functions of a PCS converter on a two-level converter-based platform. Reference [11] proposed a 3-level neutral point clamped (3L-NPC) converter based PCS converter topology. Reference [12] built one phase leg of a MMC that can work as the PCS.

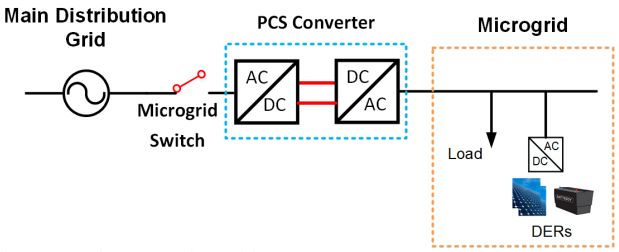

Fig. 1 Asynchronous microgrid structure.

This paper focuses on the actual controller design and implementation for a four-wire MV microgrid side PCS converter considering grid requirements. The controller is developed for a SiC MOSFET-based 13.8 kV four-wire dc/ac MMC. A modularized design is applied to assist control debugging and in the full PCS development. In the meantime, SiC MOSFET-based converter can achieve high switching frequency, which results in high noises [13] generated by the switching instants. Therefore, the noise impacts are considered in the controller design. The design and controller functions have been tested under both balanced and unbalanced load conditions in microgrid grid-connected operation.

The rest of this paper is organized as follows: Section II introduces the converter topology, basic operation principle and modelling. Section III focuses on the control architecture design; Section IV introduces the detailed controller functions. Section V provides hardware implementation and testing results under different microgrid load conditions, and conclusions are drawn in Section VI.

II. Converter Topology and Operation Principle

A. Converter Topology

MMC is a commonly used topology for high voltage (HV) and MV applications for its modularized design and reliability [14-16]. For a 13.8 kV asynchronous microgrid, a 10 kV SiC MOSFET based, 5-level MMC with half-bridge submodules is selected as the topology of the microgrid side PCS converter, which is shown in Fig. 2.

Normally, MMC topology does not require dc-link capacitors because the submodule capacitors can work as the energy storage component. However, in the asynchronous microgrid application, in the grid-connected operation, the PCS replaces the substation transformer to link the main grid and microgrid. The PCS works as the voltage source of the microgrid in the grid-connected mode to support microgrid loads. Load conditions in the microgrid can be balanced or unbalanced. Unbalanced loads require a neutral wire, which is usually provided by the delta-Yg connected substation transformer in traditional microgrids. Therefore, in an asynchronous microgrid, the neutral wire should be provided by the microgrid side PCS converter.

In an MMC, the fourth wire can be established by adding an extra phase leg [17]. However, this solution will enlarge the total converter size and greatly increase the cost. An alternative solution is to add dc-link capacitors to the MMC and split the dc-link to form the neutral.

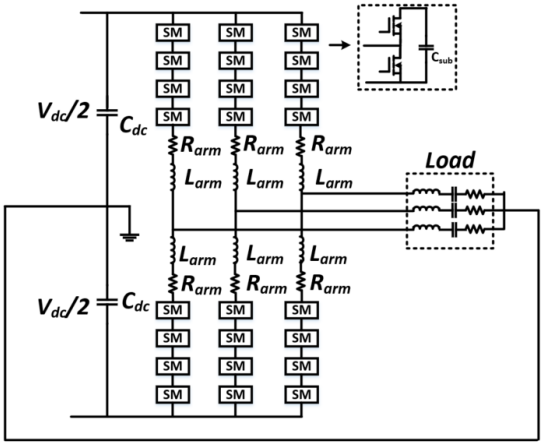

Fig. 2. Four-wire MMC topology for an asynchronous microgrid.

B. MMC Basic Operation Principle

1) Circulating Current

The equivalent circuit of one phase leg in an MMC is shown in Fig. 3. In each phase leg, there are two arms. The submodules in each arm can be modelled as a controlled voltage source. The upper and lower arm voltage is described as:

$$v_U = \frac{V_{dc}}{2} - v_{mg} - i_U R_{arm} - L_{arm}\frac{di_U}{dt} \quad (1)$$

$$v_L = \frac{V_{dc}}{2} + v_{mg} - i_L R_{arm} - L_{arm}\frac{di_L}{dt} \quad (2)$$

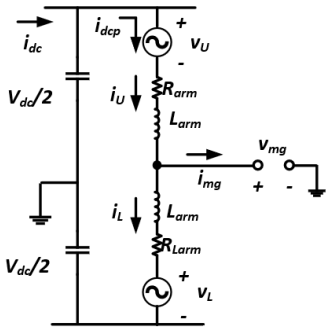

Fig. 3. Equivalent circuit for one phase leg

where L_{arm} and R_{arm} are the arm inductor parameters, v_{mg} is the microgrid ac voltage, which can be written as:

$$v_{mg} = V_{mg}\cos(wt + \psi) \quad (3)$$

The microgrid ac current is written as:

$$i_U = I_{dcp} - \frac{i_{mg}}{2} \quad (4)$$

$$i_L = I_{dcp} + \frac{i_{mg}}{2} \quad (5)$$

where I_{dcp} is the dc component in phase current. The microgrid side ac current can be written as

$$i_{mg} = I_{mg}\cos(wt + \psi + \Phi) \quad (6)$$

where $cos\Phi$ is the power factor of the ac microgrid. The instantaneous power on submodules are:

$$p_U = v_U i_U \quad (7)$$

$$p_L = v_L i_L \quad (8)$$

It is obvious that there will be second order components in the instantaneous power. According to reference [18], the second order power ripple results in second order energy ripple, eventually will cause circulating current. The circulating current is composed of even order harmonics, and the second order harmonic is the largest harmonic. Therefore, control to limit the second order harmonic is required.

2) MC Average Model

To design the ac voltage and current control, average model is usually applied. For MMC topology, it is complicated to model MMC precisely. An MMC can be modeled as a two-

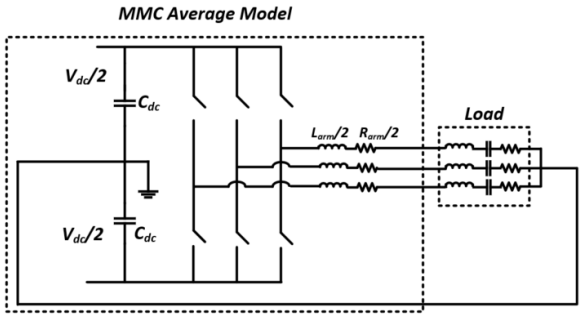

Fig. 4. Four-wire MMC average model.

level topology for the output voltage and current control [19]. In this paper, the four-wire MMC is also modeled as a four-wire two level converter, which is shown in Fig. 4. The filter impedance of the two-level model is half of the arm inductance and resistance.

III. Control Architecture Design

For the MV PCS converter, the control architecture is designed following IEEE standard 1676-2010 [20], which is shown in Fig. 5. There two main considerations for the designed control architecture: 1) modularized design; 2) compatible for full PCS.

A. Modularized Design

In the whole controller, there are three modules which are human-machine interface (HMI), central controller, and phase controllers. The three-phase converter is placed in three cabinets. Each module can be debugged independently, which can simplify the controller debugging.

The HMI is used to issue required control commands and enables/disables the whole system. For this PCS converter, the HMI is realized through LabView. The central controller is used to realize high-level control functions such as ac output voltage/current sensing and control, converter-level protection, etc. The central controller is consisting of one digital signal processor (DSP) and one field programmable gate array (FPGA). The control calculation is realized in a DSP, and the protection and communication with phase controllers are realized in a FPGA.

FPGAs are applied as the processors in phase controllers since FPGAs have better noise immunity capability compared with DSPs. Each converter cabinet has one phase controller to realize the voltage balancing control, modulation, and phase-leg protection. The phase controller design is modularized. After finishing debugging one phase controller, the other two controllers can simply duplicate the first one, which will simplify the phase controller debugging.

The central controller is connected to phase controllers with fiber optic cables. In the SiC MOSFET based high voltage PCS converter, the electromagnetic field noise is large. One advantage of the fiber optic connection is noise immunity. The communication between central and phase controllers are the serial communication in FPGAs with self-defined communication protocol.

B. Full PCS Compatiblity

Since the PCS is a back-to-back connected converter, the microgrid side PCS should be compatible for the full PCS development. Both the hardware and software are designed to be compatible for the full PCS.

From hardware perspective, an interface is designed for further full PCS operation. The interface is connected to the FPGA in the central controller and is used to link to the distribution grid side PCS converter. In the meantime, since the grid side PCS can use the same topology as the microgrid side

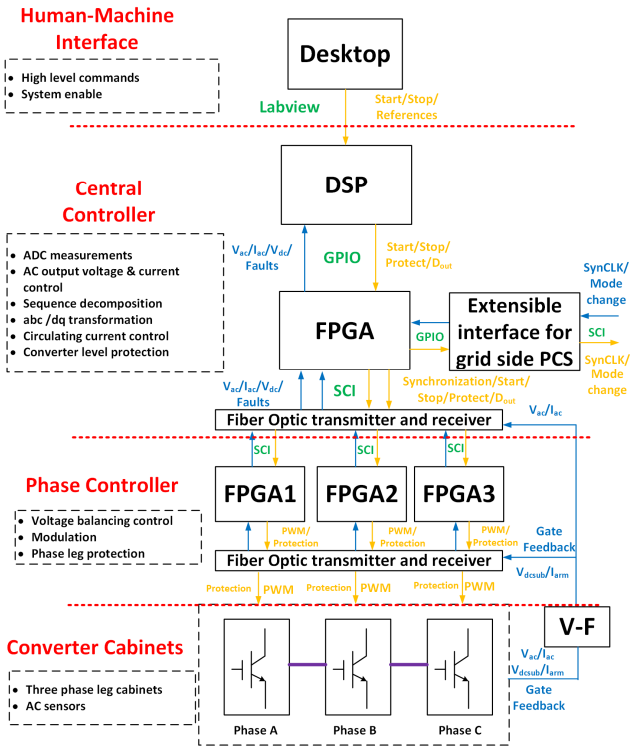

Fig. 5. Microgrid side PCS control architecture.

PCS, the designed architecture and selected hardware in the microgrid side PCS can also be used for grid side PCS.

For the software implementation, the modularized design benefits the full PCS compatibility. From control perspective, the main difference between grid side and microgrid side PCS is the central controller functions. The grid side PCS needs to regulate the dc-link voltage as well as ac current while the microgrid side PCS controls the ac output voltage and frequency. Phase controller functions for both grid and microgrid side PCS are same. Since phase controller are debugged independently, phase controllers in the microgrid side PCS can be directly applied to grid side PCS.

The grid and microgrid side PCS are connected through the extensible interfaces using fiber optic cables. Two converters will share the synchronous clock information to make the PWM signal synchronized and transfer the operation mode commands so that the converter operation mode can be changed if the asynchronous microgrid mode changes. The extensible interfaces are connected to FPGAs. The reason for this type of design is that FPGAs can provide more flexibility for the protocol design of serial communication.

IV. Controller Functions

A. Central Controller Functions

Central controller functions include two types: 1) grid required functions; 2) topology operation functions. Central controller functions are shown in Fig. 6.

1) Grid Required Function

In the grid-connected mode, the microgrid side PCS works as the source to provide voltage and frequency for the microgrid. The ac output voltage is controlled in the central controller, frequency is also provided by the PCS converter. The load condition in the microgrid could be balanced or unbalanced. Since the MMC is modelled as a two-level four-wire converter, the ac voltage control is designed based on this model. The control is realized in dq coordinates through proportional-integral (PI) controller.

2) Topology Required Function

As discussed in Section II, second order circulating current control is required for the MMC operation to reduce the submodule capacitor voltage ripple and assist voltage balancing control. The control diagram is shown in Fig. 6. The upper and lower arm current are sensed and used to calculate the circulating current in one phase. The circulating current is controlled to be zero. The control is realized in the stationary coordinates and proportional-resonant (PR) controller is used for the control [21]. The controller can also be written as (9):

$$PR(s) = K_{PR} + \frac{2K_R w_{cut} s}{s^2 + 2w_{cut} s + w_0^2} \tag{9}$$

where w_0 is the resonant frequency, which should be 240π in the circulating current control to regulate 120 Hz harmonics. The duty cycle reference calculated by the circulating current control is directly added to the duty cycle reference calculated by the ac voltage control to be the total reference duty cycle for phase controllers.

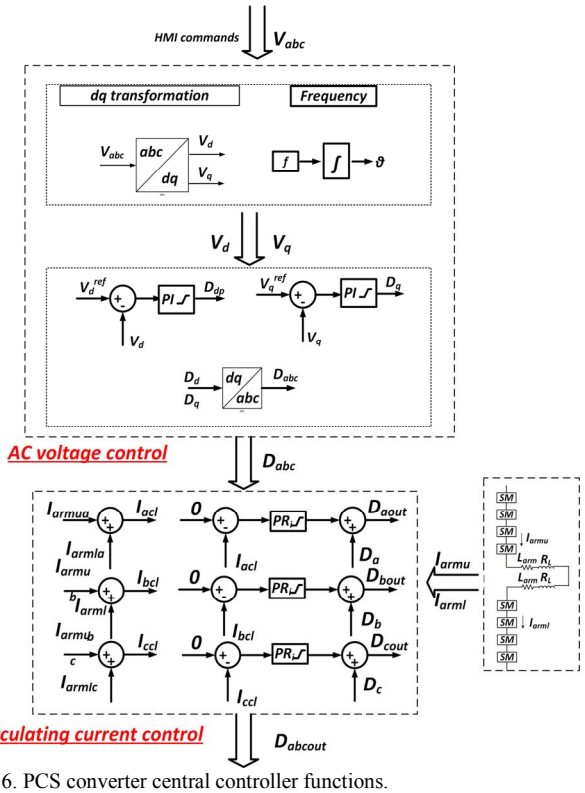

Fig. 6. PCS converter central controller functions.

B. Phase Controller Functions

The phase controller functions are shown in Fig. 7. Phase controller contains modulation, voltage balancing control, and converter protection. The submodule dc-link voltage and arm current are sent to the phase controller for the voltage sorting and modulation.

Since there are only four submodules in each arm, nearest level pulse width modulation (NLM-PWM) are applied for this microgrid PCS converter. NLM-PWM can combine the modulation and voltage balancing control together as well as reduce the low-frequency harmonics in the output voltage [22]. The detailed modulation implementation has been discussed in paper [23].

There are three kinds of protection functions which include: gate signal error protection, submodule over-voltage protection and central controller required protection. Gate drivers send feedback signals to the phase controller; once the feedback signal is abnormal, the phase controller disables gate signals. The submodule over-voltage protection is triggered when the sensed submodule voltage exceeds the maximum threshold. When the gate signal error protection or submodule over-voltage protection is triggered, the phase controller will send feedback signal to the central controller to shut down the whole system. Moreover, the protection required by the central controller is also executed in the phase controller.

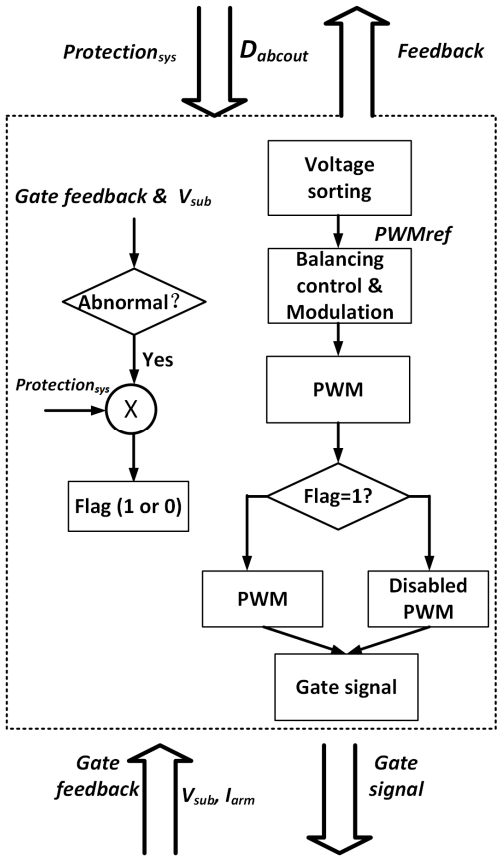

Fig. 7. PCS converter phase controller functions.

V. Hardware Implementation and Testing

A. Hardware Implementaiton

The hardware implementations of the controller are shown in Fig. 8. DSP F28335 from Texas Instrument (TI) and FPGA EP4CE22F17C6N are used as the central controller. Phase controllers are also implemented with same type of FPGAs. The central controller and phase controllers are connected through fiber optic cables. The extensive interface of the central controller is connected to the FPGA in the central controller. Fault indicators are applied on both central and phase controllers. Once the fault occurs, the controller can indicate the fault location and type, which will assist the converter testing and debugging.

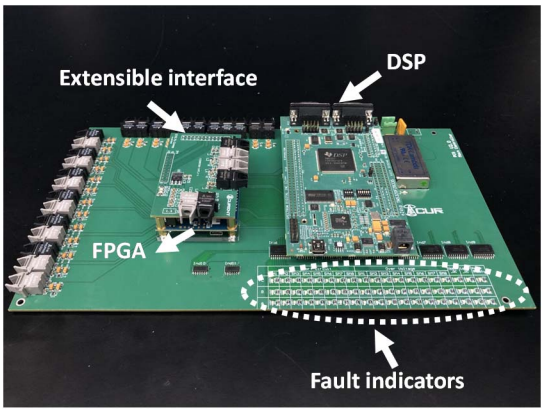

(a)

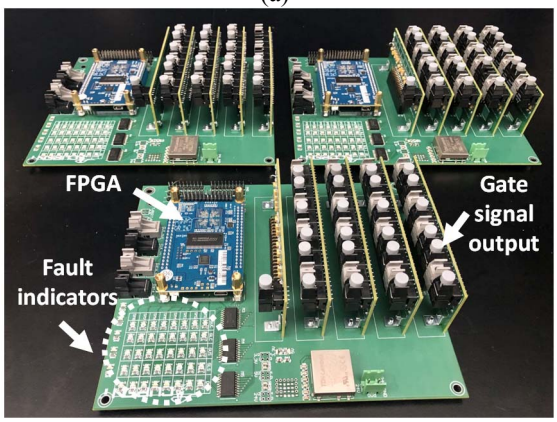

(b)

Fig. 8. Controller hardware implementation: (a) central controller; (b) phase controllers.

B. Experimental Results

The three-phase inverter setup is shown in Fig. 9. The converter is composed of three cabinets. In the grid-connected mode, the microgrid can be modelled as a load of the PCS. The converter controllers are tested under both balanced and unbalanced load conditions. The load conditions are shown in Table 1.

1) Balanced Load Condition

In the balanced load condition, the microgrid side PCS are tested at the full ac voltage 13.8 kV with 25 kV dc link voltage.

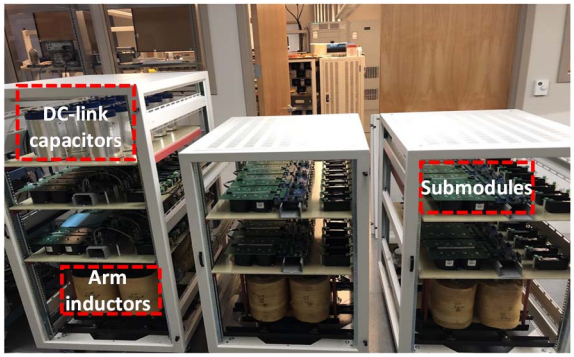

Fig. 9. PCS converter setup.

TABLE I. Full Load Operation Points

Parameters	Balanced condition	Unbalanced condition
DC-link voltage (V_{dc})	25 kV	16 kV
AC line to line voltage (V_{ac}, rms)	13.8 kV	8.8 kV
Load condition (RC in series)	R=246 Ω, C=1.25 uF	R=246 Ω C_a=C_c=1.25 uF, C_b=0.625 uF
Line frequency (f)	60 Hz	60 Hz
Arm filter (L_{arm})	L_{arm}=90 mH, R_{Larm}= 5 mΩ	L_{arm}=90 mH, R_{Larm}= 5 mΩ
Switching frequency (f_s)	10 kHz	10 kHz

The testing results are shown in Fig. 10. The submodule capacitor voltage of phase B is shown in Fig. 10 (a). The submodule capacitor voltage data comes from the phase controller. The outputs of FPGAs in phase controllers are digital data, which is transferred back to the analog data in MATLAB. The submodule voltage waveform shows that the modulation and balancing control can balance the submodule voltages. The designed phase controllers can operate normally at MV condition with high noises. The steady-state voltage and current waveform are shown in Fig. 10(b). These results demonstrate that the designed central controller works normally, and the converter can be used to support an actual 13.8 kV microgrid.

2) Unbalanced Load Condition

The unbalanced load condition is tested at ac 8.8 kV and dc 16 kV. The load setup is same as balanced load condition except the load in phase B is decreased to be 1/3. The unbalanced testing results are shown in Fig. 11. The submodule capacitor voltage of phase B is shown in Fig. 11 (a). Compared with the balanced load condition, the voltage ripple of submodules include more second order harmonics. One potential reason is the unbalanced load condition results in unbalanced phase current, the current in (6) contain negative and zero sequences components. The circulating current control in the central

controller is impacted. The ac output voltage and current waveforms are shown in Fig. 11. (b). The zero-sequence current path is provided by the fourth wire. The ac output voltage and frequency are controlled by the central controller. These results show that the four-wire PCS can support microgrids with unbalanced loads in grid-connected operation.

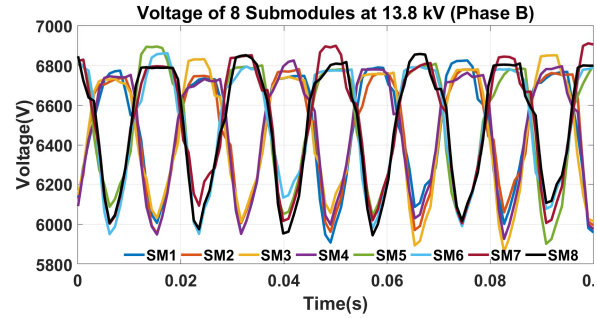

(a)

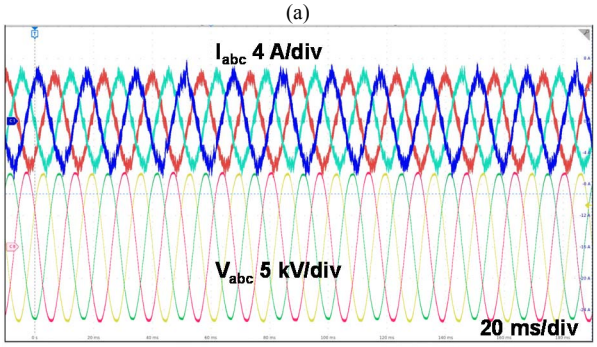

(b)

Fig. 10. Testing result for balanced load conditions: (a) submodule voltage of phase B; (b) steady-state voltage and current.

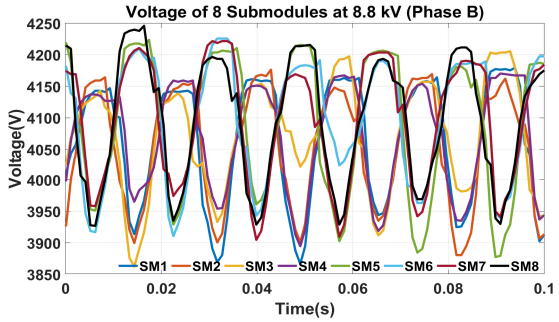

(a)

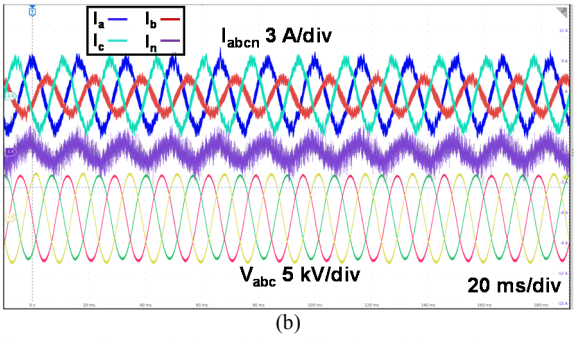

(b)

Fig. 11. Testing result for unbalanced load conditions: (a) submodule voltage of phase B; (b) steady-state voltage and current.

VI. Conclusions

In this paper, a controller has been designed and implemented in a medium voltage (13.8 kV) dc/ac converter for asynchronous microgrids. The control architecture and detailed functions in central and phase controllers are discussed. The testing results demonstrate that the designed controller can support the operation of MV microgrids under both balanced and unbalanced load conditions. The central controller can regulate the output voltage and provide stable frequency. Phase controllers can realize the modulation and submodule voltage balancing control.

However, in this paper, the unbalanced voltage control functions are not implemented and detailed impacts caused by load unbalanced are not discussed. The PCS converter operation and related controlled functions in islanded mode are also not discussed. These functions will be covered in the future work.

Acknowledgment

This work was supported primarily by DOE PowerAmerica program. This work also made use of Engineering Research Center Shared Facilities supported by the Engineering Research Center Program of the National Science Foundation and DOE under NSF Award Number EEC1041877 and the CURENT Industry Partnership Program. The authors would like to acknowledge the contribution of EPC Power, Southern Company, and Chattanooga Electric Power Board.

References

[1] V. Yaramasu and B. Wu, "Three-Level Boost Converter Based Medium Voltage Megawatt PMSG Wind Energy Conversion Systems," in *Proc. IEEE Energy Conversion Congress and Exposition* (*ECCE*), 2011, pp. 561-567.

[2] W. Chen, A. Q. Huang, C. Li, G. Wang and W. Gu, "Analysis and Comparison of Medium Voltage High Power DC/DC Converters for Offshore Wind Energy Systems," *IEEE Transactions on Power Electronics*, vol. 28, no. 4, pp. 2014-2023, 2013.

[3] X. Yuan, "A Set of Multilevel Modular Medium-Voltage High Power Converters for 10-MW Wind Turbines," *IEEE Transactions on Sustainable Energy*, vol. 5, no. 2, pp. 524-534, 2014.

[4] M. Stojadinovic and J. Biela, "Comparison of High Power Non-Isolated Multilevel DC-DC Converters for Medium-Voltage Battery Storage Applications," in *Proc. 17th European Conference on Power Electronics and Applications* (*ECCE-Europe*), 2015, pp. 1-10.

[5] X. She, A. Q. Huang, S. Lukic and M. E. Baran, "On Integration of Solid-State Transformer with Zonal DC Microgrid," *IEEE Transactions on Smart Grid*, vol. 3, no. 2, pp. 975-985, 2012.

[6] X. Yu, X. She, X. Ni and A. Q. Huang, "System Integration and Hierarchical Power Management Strategy for a Solid-State Transformer Interfaced Microgrid System," *IEEE Transactions on Power Electronics*, vol. 29, no. 8, pp. 4414-4425, 2014.

[7] M. Barnes and P. Binduhewa, "Asynchronous Interconnection of a Microgrid," in *CIRED Seminar*, Frankfurt, Germany, 2008, pp. 64-68.

[8] D. Li, S. Ji, X. Huang, J. Palmer, F. Wang and L. M. Tolbert, "Controller Development of an Asynchronous Microgrid Power Conditioning System (PCS) Converter Considering Grid Requirements," *IEEE Applied Power Electronics Conference and Exposition (APEC)*, New Orleans, LA, USA, 2020, pp. 616-621.

[9] J. Wang, N. C. P. Chang, X. Feng, and A. Monti, "Design of A Generalized Control Algorithm for Parallel Inverters for Smooth microgrid transition operation," *IEEE Transactions on Industrial Electronics,* vol. 62, pp. 4900-4914, 2015.

[10] J.-D. Park, J. Candelaria, L. Ma, and K. Dunn, "DC Ring-Bus Microgrid Fault Protection and Identification of Fault Location," *IEEE Transactions on Power Delivery,* vol. 28, pp. 2574-2584, 2013.

[11] S. Parashar, A. Kumar, and S. Bhattacharya, "High Power Medium Voltage Converters Enabled by High Voltage SiC Power Devices," in *Proc. International Power Electronics Conference (ECCE Asia)*, 2018, pp. 3993-4000.

[12] S. Ji, X. Huang, L. Zhang, J. Palmer, W. Giewont*, et al.*, "Medium Voltage (13.8 kV) Transformer-Less Grid-Connected DC/AC Converter Design and Demonstration Using 10 kV SiC MOSFETs," in *Proc. IEEE Energy Conversion Congress and Exposition (ECCE)*, 2019, pp. 1953-1959.

[13] S. Ji *et al*., "Impact of Submodule Voltage Sensor Noise in 10 kV SiC MOSFET Modular Multilevel Converters (MMCs) under High dv/dt Environment," *IEEE Applied Power Electronics Conference and Exposition (APEC)*, New Orleans, LA, USA, 2020, pp. 1089-1093

[14] M. Yan, Z. Zhang, Z. Xu, L. Chen, G. Cheng and Q. Wang, "Comparative Study on DC Line Fault Transient Characteristics of Four Typical MMC-HVDC Configurations," *IEEE PES Asia-Pacific Power and Energy Engineering Conference (APPEEC)*, Macao, Macao, 2019, pp. 1-5.

[15] M. Alharbi, S. Isik and S. Bhattacharya, "Reliability Comparison and Evaluation of MMC Based HVDC Systems," *IEEE Electronic Power Grid (eGrid)*, Charleston, SC, 2018, pp. 1-5.

[16] G. Tang, Z. Xu and Y. Zhou, "Impacts of Three MMC-HVDC Configurations on AC System Stability Under DC Line Faults," in *IEEE Transactions on Power Systems*, vol. 29, no. 6, pp. 3030-3040, Nov. 2014.

[17] H. M. P. and M. T. Bina, "A Transformerless Medium-Voltage STATCOM Topology Based on Extended Modular Multilevel Converters," in *IEEE Transactions on Power Electronics*, vol. 26, no. 5, pp. 1534-1545, May 2011.

[18] Qingrui Tu, Zheng Xu, H. Huang and Jing Zhang, "Parameter design principle of the arm inductor in modular multilevel converter based HVDC," *International Conference on Power System Technology*, Hangzhou, 2010, pp. 1-6.

[19] H. Wu, X. Wang, Ł. Kocewiak and L. Harnefors, "AC Impedance Modeling of Modular Multilevel Converters and Two-Level Voltage-Source Converters: Similarities and Differences," *IEEE 19th Workshop on Control and Modeling for Power Electronics (COMPEL)*, Padua, 2018, pp. 1-8.

[20] *IEEE Guide for Control Architecture for High Power Electronics* (*1 MW and Greater*) *Used in Electric Power Transmission and Distribution Systems*, IEEE Std. 1676-2010, 2011.

[21] S. Li, X. Wang, Z. Yao, T. Li and Z. Peng, "Circulating Current Suppressing Strategy for MMC-HVDC Based on Nonideal Proportional Resonant Controllers Under Unbalanced Grid Conditions," in *IEEE Transactions on Power Electronics*, vol. 30, no. 1, pp. 387-397, Jan. 2015.

[22] Y. Wang, C. Hu, R. Ding, L. Xu, C. Fu and E. Yang, "A Nearest Level PWM Method for the MMC in DC Distribution Grids," in *IEEE Transactions on Power Electronics*, vol. 33, no. 11, pp. 9209-9218, Nov. 2018.

[23] S. Ji, L. Zhang, X. Huang, J. Palmer, F. Wang and L. M. Tolbert, "A Novel Voltage Balancing Control with dv/dt Reduction for 10 kV SiC MOSFET Based Medium Voltage Modular Multilevel Converter," in *IEEE Transactions on Power Electronics.*